City Research Online

City, University of London Institutional Repository

This is the published version of the paper.

This version of the publication may differ from the final published version.

RESEARCH ARTICLE

Computational prediction of electrical and thermal properties of graphene and BaTiO3 reinforced epoxy nanocomposites

Raghvendra Kumar Mishra[1], Saurav Goel[2,3,4,5*] and Hamed Yazdani Nezhad[6*]

[1] School of Aerospace, Transport and Manufacturing, Cranfield University, MK430AL, United Kingdom

[2] School of Engineering, London South Bank University, London, SE10AA, United Kingdom

[3] Shiv Nadar University, Gautam Budh Nagar, 201314, India

[4] Indian Institute of Technology Guwahati, Guwahati, 781039, India

[5] University of Petroleum and Energy Studies, Dehradun, 248007, India

[6] Department of Mechanical Engineering and Aeronautics, City University of London, Northampton Square London, EC1V0HB, United Kingdom

* Correspondence emails: goeLs@Lsbu.ac.uk and hamed.yazdani@city.ac.uk

ABSTRACT

Graphene based materials e.g., graphene oxide (GO), reduced graphene oxide (RGO) and graphene nano platelets (GNP) as well as Barium titanate (BaTiO3) are emerging reinforcing agents which upon mixing with epoxy provides composite materials with superior mechanical, electrical and thermal properties as well as shielding against electromagnetic (EM) radiations. Inclusion of the these reinforcing agents shows improved performance; however, the extent of improvement has remained uncertain. In this study, a computational modelling approach was adopted using COMSOL Multiphysics software in conjunction with Bayesian statistical analysis to investigate the effects of including various filler materials e.g., GO, RGO, GNP and BaTiO3 in influencing the direct current (DC) conductivity (σ), dielectric constant (ε) and thermal properties on the resulting epoxy polymer matrix composites. The simulations were performed for different volume percentage of the filler materials by varying the geometry of the filler material. It was observed that the content of GO, RGO, GNPs and the thickness of graphene nanoplatelets can alter the DC conductivity, dielectric constant, and thermal properties of the epoxy matrix. The lower thickness of GNPs was found to offer the larger value of DC conductivity, thermal conductivity and thermal diffusivity than rest of the graphene nanocomposites, while the RGO showed better dielectric constant value than neat epoxy, and graphene nanocomposites. Similarly, the percentage content and size (diameter) of $BaTiO_3$ nanoparticles were observed to alter the dielectric constant, DC conductivity and thermal properties of modified epoxy by several order of magnitude than neat epoxy. In this way, the higher diameter particles of $BaTiO_3$ showed better DC conductivity properties, dielectric constant value, thermal conductivity and thermal diffusivity.

Introduction

Polymer composites and nanocomposites are made up of more than one phase or reinforcement (e.g. nanomaterials or fibres) (K. S. Cho, 2016; Marsden et al., 2018; Mather et al., 2009; McGrail et al., 2015), possessing properties better than pristine materials if tailored with proper engineering (K. S. Cho, 2016; Marsden et al., 2018; Mather et al., 2009; McGrail et al., 2015). A vast majority of polymers (with no additional phase or reinforcement added) are largely insulating [3], e.g. epoxy polymers. This limits theirwider applications in high-value manufacturing i.e., aerospace (Friedrich & Almajid, 2013; Marsden et al., 2018; Oladele et al., 2020), automotive (K. S. Cho, 2016; Marsden et al., 2018;

Mather et al., 2009; McGrail et al., 2015), energy (Friedrich & Almajid, 2013; Marsden et al., 2018; Oladele et al., 2020) and biomedical applications (Friedrich & Almajid, 2013; Marsden et al., 2018; Oladele et al., 2020). Introducing additives or fillers into the polymer matrix enhances the performance of the composites by improving their conduction, lightning strike protection (Korattanawittaya et al., 2017; Li et al., 2017; Marra et al., 2016; Ming et al., 2015), electromagnetic shielding (Korattanawittaya et al., 2017; Li et al., 2017; Marra et al., 2016; Ming et al., 2015), anti-static components (Korattanawittaya et al., 2017; Li et al., 2017; Marra et al., 2016; Ming et al., 2015), as well as strain energy (Korattanawittaya et al., 2017; Li et al., 2017; Marra et al., 2016; Ming et al., 2015) which are vital properties required in the aerospace sectors to fabricate next-generation composite materials (Korattanawittaya et al., 2017; Li et al., 2017; Marra et al., 2016; Ming et al., 2015).

Carbon-based fillers (mainly carbon nanotubes (CNTs) and carbon black (CB)) can lead to excellent conductive properties in composites due to their superior electrical, thermal conductivity as well as decent mechanical properties (Caradonna et al., 2019). Presently, graphene has drawn considerable scientific interest as a potential conductive filler material. Graphene is a 2D sheet of sp^2 bonded carbons in a hexagonal network with outstanding electrical conductivity of 6×10^5 S m^{-1} (Lewis et al., 2019). Recently, there has been an emergence of a group of graphene-based materials (GRMs) ranging from pristine (ideal) graphene, graphene nanoplatelets, (GNPs), or distinct chemical structures such as graphene oxide (GO) (Zandiatashbar et al., 2014). The morphological variations among GRMs as well as pristine graphene dramatically affect the functionality of the polymer-based nanocomposites (Hass et al., 2008). Currently, the graphene-thermoplastic polymer-based nanocomposites have shown excellent strength as well as electrical conductivity, including graphene-epoxy nanocomposites (Pathak et al., 2016) as well as the GO–thermoplastic nanocomposites (Carotenuto et al., 2012). As such graphene on its own has a high intrinsic thermal and electrical conductivity at room temperature (RT) (Hass et al., 2008). It is interesting to note that while the thermal conductivity of composites improves by inclusion of thermal conducting fillers, however, the thermal percolation in composites becomes an issue (Lewis et al., 2019). Research shows that thermal percolation threshold does not occur at all (Shahil & Balandin, 2012b). It is also shown that even the inclusion of a little fraction of graphene fillers can enhance the electrical and thermal conductivity of as-received epoxy composites (Marsden et al., 2018; McGrail et al., 2015) from 0.2 W/mK to 2.2 W/mK which shows an improvement by 1000% (10^3 order). Numerous ongoing research studies on the electrical and thermal properties of composites with higher content of graphene fillers have revealed that the mixing conditions (referred to as loading conditions) plays a vital role in enhancing the thermal conductivity (Carotenuto et al., 2012; Hass et al., 2008; Zandiatashbar et al., 2014).

The objective of this research paper is to numerically estimate the DC conductivity, dielectric and thermal characteristics of Epoxy/GNP and Epoxy/BaTiO3 nanocomposites as a function of filler content using finite element (FE) analysis (Bikky et al., 2010) in conjunction with the Bayesian statistical analysis. To do so, a geometric model made of uniformly distributed nanofillers was developed which was subjected to a static-electric current and heat transfer solver in the AC/DC module of COMSOL Multiphysics® v5.5 (Bikky et al., 2010; Chikhi et al., 2013). The resulting data was treated with Bayesian approach to ascertain the sensitivity in the approximated values which was benchmarked to the literature wherever possible.

Literature review

In the past, a myriad of studies are conducted to evaluate the electrical conductivity of epoxy composites. A summary of these studies has been shown in Table 1 and Table 2.

"Resin material"	"Filler material"	Electrical conductivity (S/m)	Fabrication Process
Epoxy (Caradonna et al., 2019)	1.0 wt% MWCNT	0.121	Three rolls mill
Epoxy (Caradonna et al., 2019)	30 wt% GNPs	0.161	Three rolls mill (Caradonna et al., 2019) (Caradonna et al., 2019)(Caradonna et al., 2019)(Caradonna et al., 2019)(Caradonna et al., 2019)
Vinyl –ester (Marra et al., 2016)	3.0 wt% GNPs	2.93	Mechanical stirring and sonication
Epoxy (Marra et al., 2016)	12 wt% GNPs	23	Vacuum Assisted
Epoxy (Marra et al., 2016)	24 wt% GNPs	56	Vacuum Assisted
Natural Rubber(Korattanawittaya et al., 2017)	10 vol% GNPs	15	Magnetic stirrer

Resin material	Filler material		Processing
Epoxy(Atif et al., 2016)	0.52 vol%GNPs	0.05	Solution blending
Epoxy(Zhao et al., 2016)	0.16 vol%GNP	10	Solution blending
Epoxy(Yousefi et al., 2014)	0.12 vol%rGO	1	Solution blending
Epoxy(Tang et al., 2014)	0.78 vol%f-GO	1	Solution blending

Table 1: Electrical conductivity values of epoxy nanocomposites obtained from various processes (In table 1, MWCNT means Multi walled carbon nanotubes, GNP means graphene nanoplatelets and GO means graphene oxide).

"Resin material"	"Filler material"	Thermal conductivity (W/mk)	Processing
Epoxy(Kargar et al., 2018)	10.0 vol% GNPs	0.7	-
Epoxy(Lewis et al., 2019)	21.8/21.8 vol% (GNPs/h-BN)	6.5	-
Epoxy(Lewis et al., 2019)	21.8/1 vol% (GNPs/h-BN)	4.7	-
Epoxy(Hou et al., 2018)	6.0 wt% GNPs	10	-
Epoxy(Jarosinski et al., 2017)	4.0 wt% GNPs	0.45	-
Epoxy(Gresil et al., 2017)	10.0 wt% GNPs	0.7	Mapping
Epoxy(Shahil & Balandin, 2012a)	10.0 vol% GNPs	5.1	-
Epoxy(Galpaya et al., 2012)	3.8 wt% GNPs	1.6	-

Table 2: Thermal conductivity of various epoxy nanocomposites.

Dielectric materials having ability to hold dielectric field strength during substantial dielectric loss, are backbone to the microelectronic device-structures (Zepu Wang et al., 2012). Nevertheless, their low dielectric permittivity (ε) limits their applications (Popielarz & Chiang, 2007), implying that the dielectric permittivity enhancement of a two-phase composite material is highly desirable. While the addition of higher filler content is known to improve its dielectric permittivity, it can negate the flexibility and other mechanical properties (Kultzow & Mainguy, 2001). On the other hand, Barium titanate (BaTiO₃) is a perovskite type electro-ceramic nanomaterial that offers superior dielectric constant in addition to ferro-, piezo- and pyro-electric features. Several researchers have studied BaTiO3

enhanced polymer nanocomposites and found superior dielectric, piezoelectric and ferroelectric properties (Tomer et al., 2010), primarily those with extremely high BaTiO3 loading (Pant et al., 2006). A relatively low content BaTiO3 in the polymer composite can also aid to provide in-situ sensing for probing mechanical behaviour of the composite material (Barber et al., 2009). The dielectric permittivity of the polymer composite based on ceramic fillers is usually controlled by the increasing content of the ceramic nanomaterials (Pant et al., 2006). A summary drawn from the literature on the dielectric constant of BaTiO3/epoxy nanocomposites is summarized in Table 3.

Resin	Fillers	Dielectric constant	Method of investigation used
Epoxy (Luo et al., 2017)	0.3 vol% BaTiO₃	210	Modeling
Epoxy (Cho et al., 2005)	0.6 vol% BaTiO3 (442nm)	65	Experimental
Epoxy (S. D. Cho et al., 2005)	0.6 vol% BaTiO3 (78nm)	25	Experimental
Epoxy (Phan, Chu, Luu, Nguyen Xuan, Pham, et al., 2016)	0.7 vol% BaTiO3 (160)	60	Modeling
Epoxy (Phan, Chu, Luu, Nguyen Xuan, Pham, et al., 2016)	0.6 vol% BaTiO3 (1000)	70	Modeling
Epoxy (Phan, Chu, Luu, Nguyen Xuan, Martin, et al., 2016)	5.0 wt% BaTiO3 (not nano)	4.01	Experimental
Epoxy (Phan, Chu, Luu, Nguyen Xuan, Martin, et al., 2016)	10.0 wt% BaTiO3 s (not nano)	7.5	Experimental
PDMS(Z. Wang et al., 2011)	0.43 vol% GNPs	11	Modelling
Epoxy(Kim et al., 2016)	10.0 vol% BaT (not nano)	26	Experimental
PVDF(Zhang et al., 2016)	0.4 vol% BaT-Fe304	140	Modelling and Experimental

Table 3: The dielectric constant of dielectric enhanced BaTiO₃/epoxy nanocomposites.

Numerical modelling has always been a preferred choice of method for investigation when it concerns predictive nature of the work in a wide array of combinations. In this aspect, COMSOL Multiphysics has a conventional physics-based user interface which solves variety of partial differential equations. In the past, COMSOL has been used to investigate the capacitance and dielectric properties

(Ekanath et al., 2011; Schumacher et al., 2009). Similarly, researchers have also analysed the distribution of electric field in dielectric nanocomposites comprising a core-shell structure by phase-field modelling method (Mekala & Badi, 2013). Further studies have been conducted on dielectric behaviour of spherical core and shell structure in core-shell structure (Mekala & Badi,

2013). However, a concentrated effort on understanding the influence of filler material such as graphene and BaTiO₃ based epoxy nanocomposite is not evident in the extant literature. This becomes the key to use COMSOL modelling based methodology in this work.

Methodology

The investigation in this work began by first modelling the geometry of the epoxy-based nanocomposite models using SolidWorks®. The models were developed with a set of assumptions stated below with varying contents of nanofillers (GNP and BaTiO3), as shown in Figure 1. The assumptions considered in the development of the model were:

- The bonding between the filler and the epoxy material was coherent, defect-free and the particles in the epoxy were tightly attached to each other.
- The filler material was dispersed homogenously and uniformly having the same particle size
- Size of the filler particle was considered spherical
- The geometry was considered non-porous (continuum) and to follow the Linear solid elastic materials compliance
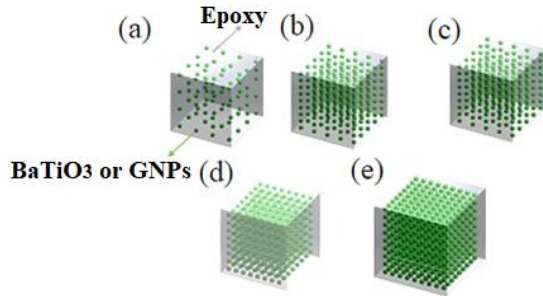

Figure 1. Model for GNP and BaTiO₃ embedded nanocomposite; a) 1.0 vol% b) 3.0 vol%, c) 5.0 vol%, d) 7.0 vol%, e) 10.0 vol%.

3.1. Boundary conditions used to model electrical properties

Electro-static analytical formulae were used to measure the DC conductivity by using Ohm's Law (Bauhofer & Kovacs, 2009). The electro-static model was established in the AC/DC module of COMSOL Multiphysics 5.5. The DC conductivity was estimated by the direct relationship between electrical conductivity and electrical field, and similarly, the dielectric constant was measured by the relationship between relative permittivity, dielectric constant and electric field, given by the following equations: (Bauhofer & Kovacs, 2009).

$$J = \sigma E \qquad (1)$$

$$E = - \nabla V \qquad (2)$$

where σ is conductivity of the material (either fillers or matrix), E, ∇V and J are the applied electric field, potential difference and electric current density, respectively.

Figure 2 shows a schematic illustration of the boundary condition applied to carry out the electrostatic simulations to simulate epoxy/BaTiO₃ and epoxy/GNPs nanocomposites.

A careful optimisation of the prior work revealed that the most suitable boundary conditions were:

(a) Reference impedance (fixed) of 50 ohms
(b) Electric insulation was applied on all the faces except ground and terminal. The insulation condition is shown in equation (3). Ground boundary condition was employed on one side of the composite element as the applied voltage of 0V (Ground 2) and terminal's boundary condition were applied on the other side of composite by the applied voltage of 230 V (Terminal 1). The stationary equation was used to perform this simulation, in this case, a steady-state problem in which the voltage does not change with time and thus the terms with time derivatives were not used:

$$nJ = 0 \qquad (3)$$

The distributed capacitance of the composite system was simulated in COMSOL 5.5 Multiphysics dielectric constant model, which can be expressed as:

$$D = \text{€}_0 \text{€}_r E \qquad (4)$$

wherein *E* is the applied electric field, and € and €r are the relative permittivity of reinforcement, matrix and permittivity of vacuum.
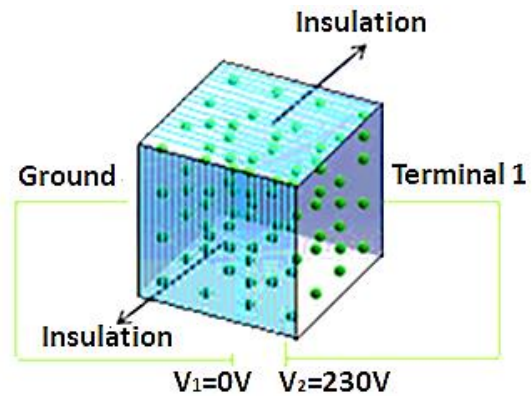

Figure 2. A free body diagram of the electrostatic simulation revealing the boundary conditions

The 3D-rectangular (tetrahedral) mesh with extra fine grain was used to perform the simulation available within the COMSOL Multiphysics 5.5 software. This meshing condition for simulation was employed based on mesh sensitivity criteria and it was found that the simulation was sensitive to the meshing size and type, and there was little variation in properties with respect to the different mesh and meshing size, as shown in Figure 3. The average value of the properties was taken with respect to different meshing types and the properties were roughly related to 3D-rectangular (tetrahedral) mesh with extra fine grain, therefore, 3D-rectangular (tetrahedral) mesh with extra fine grain was used to complete the simulation.
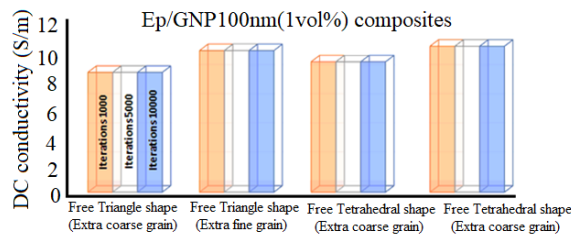

Figure 3. The DC conductivity of GNPs with thickness of (100 nm) and Epoxy (Ep) composites with various types of mesh and element size

2.2. Boundary conditions used to model thermal properties

Temperature can be regarded as analogous to electrical potential as in their gradient led to a flow of heat or electrical current respectively. While heat flows from a higher temperature to a lower temperature heat conduction occurs as a result of the phonon vibration depending on the thermal conductivity of the material (akin to electrical conductivity of the material). The heat transfer Module of COMSOL Multiphysics 5.5 facilitates essential heat transfer mechanisms such as conduction and convection, in addition to radiative heat transfer. The temperature-based equation can be described throughout solid domains which is compliant with the Fourier's law of conduction. Theoretically, the conduction within the solid medium, follows Fourier's law of heat conduction expressed by the conductive heat flux (q), which is proportional to the temperature gradient (∇T(K)), and the thermal conductivity (k W/(m·K)) expressed as (R. Byron Bird Warren E. Stewart Edwin N. Lightfoo et al., 2006):

$$q = -k\nabla T \qquad (5)$$

Additionally, the thermal properties were estimated by the heat transfer at the solids interfaces $\rho c_p u_{trans}.\nabla T + \nabla.q = Q$ which can be derived from Equation (5) (R. Byron Bird Warren E. Stewart Edwin N. Lightfoo et al., 2006) where *Cp*, ∇q *and*

u_{trans} are the specific heat capacity (J/kg·K), change in heat flux by conduction (W/m^2) and velocity vector of translational motion (m/s) respectively. The boundary conditions used were (a) fixed reference temperature of 293.15 K; (b) thermal insulation was applied on all the faces except initial temperature and terminal temperature as shown in Figure 4; the initial temperature of 293.15 K (T_1) was applied on one side of the composite element; the terminal temperature of 393.15 K (T_2) (Terminal 1) was applied on the other side of the element. (c) The stationary equation used to perform the heat transfer simulation was based on the insulation condition which is expressed as nq=0 where n is scalar quantity and q is heat transfer.
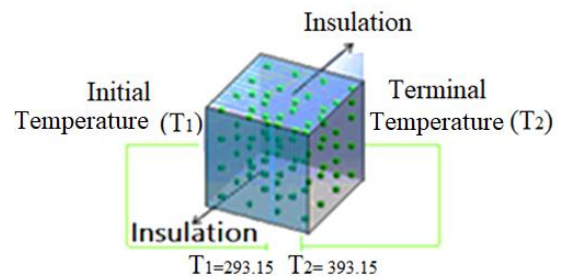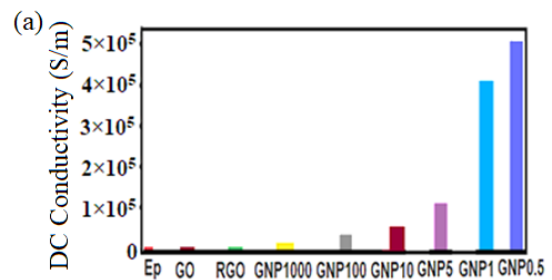

Figure 4. A free body diagram showing the boundary conditions used for heat transfer simulation. Temperature is shown in Kelvin

Results

4.1. Simulated DC conductivity of GNP embedded epoxy nanocomposite

In this context, carbon-based conductive nanofillers, such as GNP continue to receive greater consideration in flexible electronics because of their flexibility as well as low electrical resistance. Throughout the simulations, various graphene compositions (e.g., graphene oxide (GO), reduced graphene oxide (RGO) and GNP (GNP1000, GNP100, GNP10, GNP5, GNP1, GNP0.5) were used as nanofillers with the epoxy matrix (Ep). The disparity amongst different types is apparent from the FE solutions. The FE solution for electrical conductivity, as well as the dielectric constant for all the graphene based compositions are shown in Figure 5a and 5b.
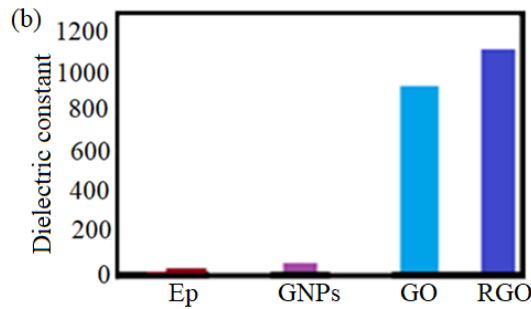
Figure 5. The DC conductivity for various types of GNPs a) DC conductivity of epoxy, graphene oxide (GO), reduced graphene oxide and various GNPs with thickness of (1000 nm, 100 nm, 10 nm, 5 nm, 1 nm, 0.5 snm), **b)** Dielectric constant of epoxy, graphene oxide (GO), reduced graphene oxide and GNPs.

Figures 6(a) and (b) shows the FE estimated values of the DC conductivity for the graphene embedded epoxy nanocomposites benchmarked to pure epoxy and pure graphene oxide without any mixing. Fig. 6 highlights that the DC conductivity of epoxy/ GO composites and the DC conductivity of epoxy/GO composites is higher than the neat epoxy, however, the DC conductivity value for epoxy/GO composites is very low, it is due to the poor conductivity nature of graphene oxide. Fig. 6b suggests that DC conductivity of RGO and GNPs based composites show higher DC conductivity than the neat epoxy and epoxy/ GO composites due to better conductivity of GNPs and RGO than GO. Additionally, a higher value for DC conductivity in epoxy composites can be achieved by having a higher thickness of graphene nanoplatelets. The increases in the DC conductivity is tied with higher vol.%. The maximum increase in the DC conductivity was achieved for 1 nm thickness of GNPs. The higher conductivity of composites with lower thickness of graphene (e.g., 1 nm thickness) confirms ballistic conductivity of graphene nanopalates, ballistic conductivity leads to electrical conduction with negligible scattering of electron. Moreover, overall conductivity of polymer composites is owing to the tunneling mechanism of electron, wherein, fillers conducting network of fillers provide the electron through the insulation matrix.
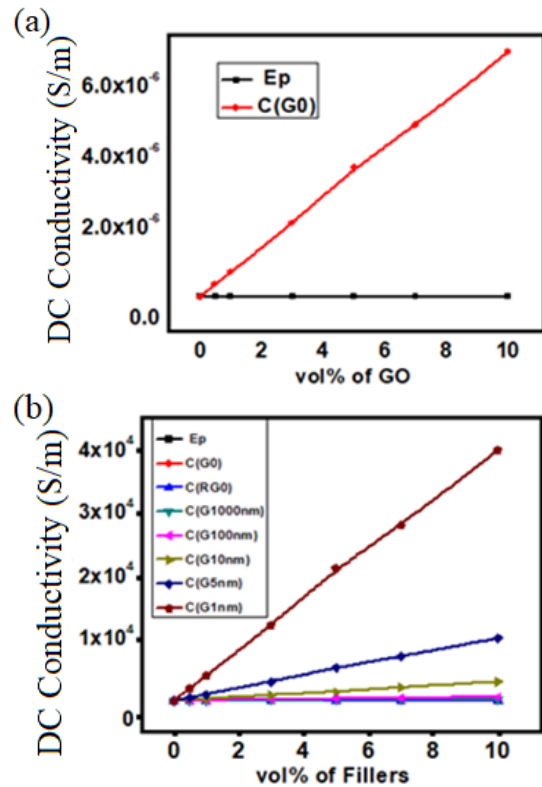

Figure 6. The FE solution for DC conductivity of various GNPs/Epoxy composites: **a)** DC conductivity of neat epoxy and epoxy/ graphene oxide (GO), b) DC conductivity of reduced graphene oxide and various GNPs with respect to thickness (1000nm(G1000nm), 100nm(G100nm), 10nm(G10nm), 5nm(G5nm), 1nm(G1nm)) composites.

Figure 7a shows the FE estimates of the dielectric constant of graphene-enhanced nanocomposites. As shown in Figure 7a and b, the dielectric constant of composites-containing various graphene-enhanced increases linearly with graphene percentage from 0.2 to 10.0 vol%. All samples of reduced graphene oxide (RGO) exhibited a pronounced improvement in the dielectric constant in comparison to the others type of graphene-based nanocomposites at the similar filler content (Figure 7(b)). From Figure 7, it can also be seen that the graphene content and composition have greater effects on the dielectric constant of the composites which can be attributed to the accumulation of charges. Also, the dielectric constant of the composites formulated by GNP-epoxy composites showed negligible dependency on the thickness of GNP. Hence, the selection of graphene in a polymer matrix needs to carry suitable consideration to choose appropriate dielectric constant of the types of graphene and thickness of graphene nanoplatelets (GNPs).
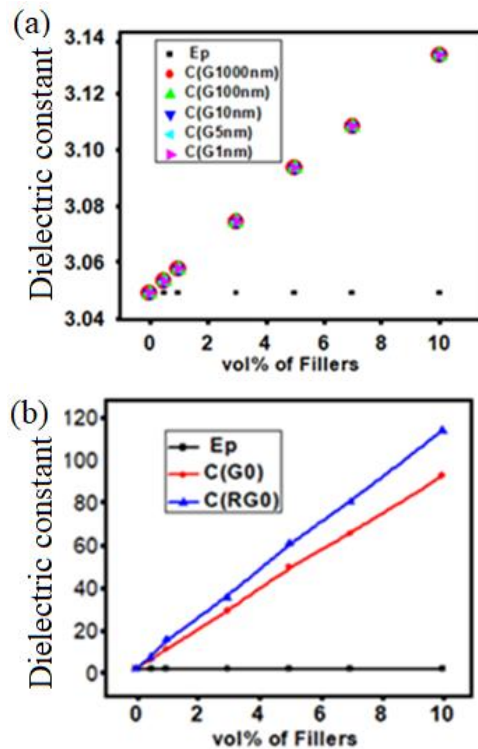
Figure 7. The FE solution for the dielectric constant of a) epoxy/ various GNPs with respect to thickness (1000nm, 100nm, 10nm, 5nm, 1nm) nanocomposites, b) epoxy/ graphene oxide (GO), reduced graphene oxide composites.

4.2. Simulated DC conductivity of BaTiO₃/epoxy nanocomposites

This section details the simulated results of the DC conductivity and the dielectric constant of epoxy/BaTiO₃nanocomposites. The electrical conductivity of neat epoxy and epoxy composites having different contents of BaTiO₃ is shown in Figure 8(a). The approximated electrical conductivity of BaTiO₃-epoxy composites was seen to increase by increasing the content of BaTiO₃ filler material. The enhancement in electrical conductivity of BaTiO₃-epoxy composites may be related to the development of conductive paths with higher BaTiO₃ content. Therefore, the conductivity of epoxy/BaTiO3 composites is higher than pure epoxy, however, the conductivity of BaTiO₃ is very little in comparison to other conducting nanofillers, as, the neat epoxy and BaTiO₃ exhibits an electrical conductivity of the order of 1.0×10^{14} s/m and 1.0×10^{9} s/m respectively. The dielectric constant of various BaTiO₃ particles (e.g. different diameter) is presented in Figure 8(b). It showed that there is a correlation between dielectric constant and crystal structure of BaTiO₃ due to the expansion of lattice caused by decreasing particle size.

BaTiO₃ as a dielectric material offers dielectric as well as charge storage capacity to the polymer matrix. Dielectric constant associated with material

is an aspect which reveals the charge storage capability of BaTiO₃-epoxy composites under an applied external electric field. The dielectric constant of BaTiO₃-epoxy composites as shown in Figure 8(c) also provides an identical trend for different diameter particles of BaTiO₃. It was found that the dielectric constant of all the samples (BaTiO₃-epoxy composites) is higher than the corresponding neat epoxy. Regarding nanocomposites, the improvement of dielectric constant can be attributed to the orientation of dipoles, which is highly constrained at the BaTiO₃-epoxy interfacial area. As a result there occurs an increase in the dielectric constant through the accumulation of free charges at the interface of epoxy and BaTiO₃ composites.
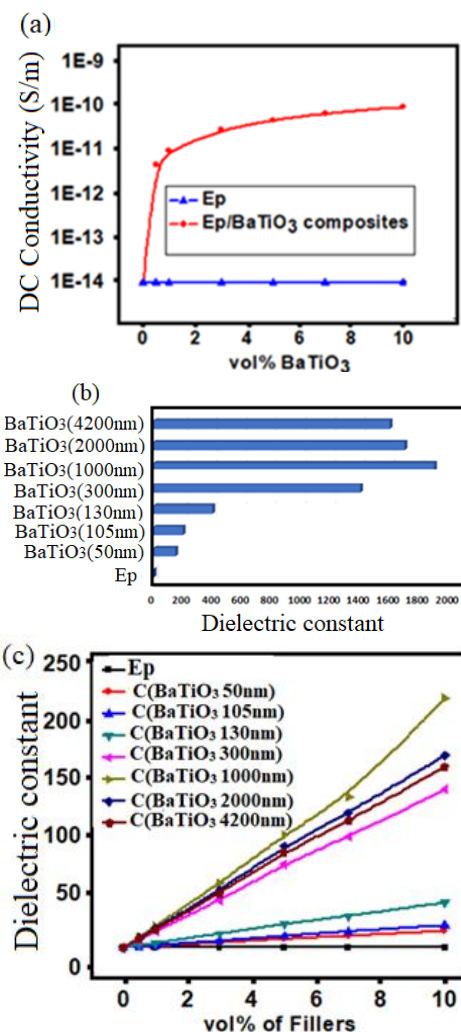

Figure 8. a) DC conductivity of BaTiO₃/Epoxy composites compared with pure epoxy, b) Dielectric constant of various BaTiO₃ with respect to the various particle diameters of BaTiO₃ (50nm, 105 nm, 130 nm, 300 nm, 1000 nm, 2000nm, 4200 nm), c) Dielectric constant of various BaTiO₃/ Epoxy composites in various filler percentages.

4.3. Simulated thermal conductivity of GNPs embedded epoxy nanocomposites

Generally, the thermal conductivity of nanocomposites is dependent on the structure, loading quantity of fillers and thermal properties of the fillers. The thermal conductivity of all the GNPs and neat epoxy is shown in Figure 9a. Figure 9b shows the resultant thermal conductivity of graphene/epoxy nanocomposites. The GNP0.5 /epoxy nanocomposites showed the highest value of thermal conductivity, however, the GO, RGO and epoxy showed lower thermal conductivity in comparison to the graphene nanoplatelets. The increasing in the thermal conductivity with a greater volume proportion of graphene is related to various states of graphene and thickness of graphene nanoplatelets. These results show a trend for the thermal conductivity in epoxy composites with respect to different structural changes of graphene, meanwhile, an increasing thermal conductivity with respect to the increasing filler proportion for the graphene/epoxy nanocomposites was found similar in all the cases. It confirms that the thermal conductivity is highly sensitive to the structural transformation and nanoscale has impact on the thermal conductivity due to ballistic conductivity at the nanoscale (e.g., less loss of heat during the conduction because of lesser scattering in phonon vibration at nanoscale).

Using the same simulation framework, the specific heat capacity of various materials were also extracted (see figure 9c). Specific heat capacity is defined as the heat required to increase (or decrease) the material temperature by one degree. Figure 9d shows the specific heat capacity of various nanocomposites as a function of thickness of graphene nanoplatelets benchmarked to pure epoxy. From Figure 9d, the specific heat capacity of composites-including different types of graphene can be seen to decrease as the content of graphene fillers vary from 0.2% to 10.0 vol%, although, graphene-based composites showed a lower specific heat capacity value in comparison to the neat epoxy. Hence, it can be concluded that graphene has an influence on the specific heat capacity of composite and there is less delay in the rise of temperature of a composite due to lower specific heat and excellent thermal conductivity of graphene.

Figure 9e shows thermal diffusivity changes in various types of composites simulated. The thermal diffusivity showed a decreasing trend with the increase in filler content. However, thermal diffusivity of composite samples from graphene with different thickness/ epoxy showed an increasing tendency of thermal diffusivity (from lower to higher thickness) with increasing filler content. It proves that higher thermal diffusivity can be

obtained by the greater mean free path of phonon-phonon, it is owing to the mean free path of phonon-phonon and thermal conductivity and specific heat of nanofillers.
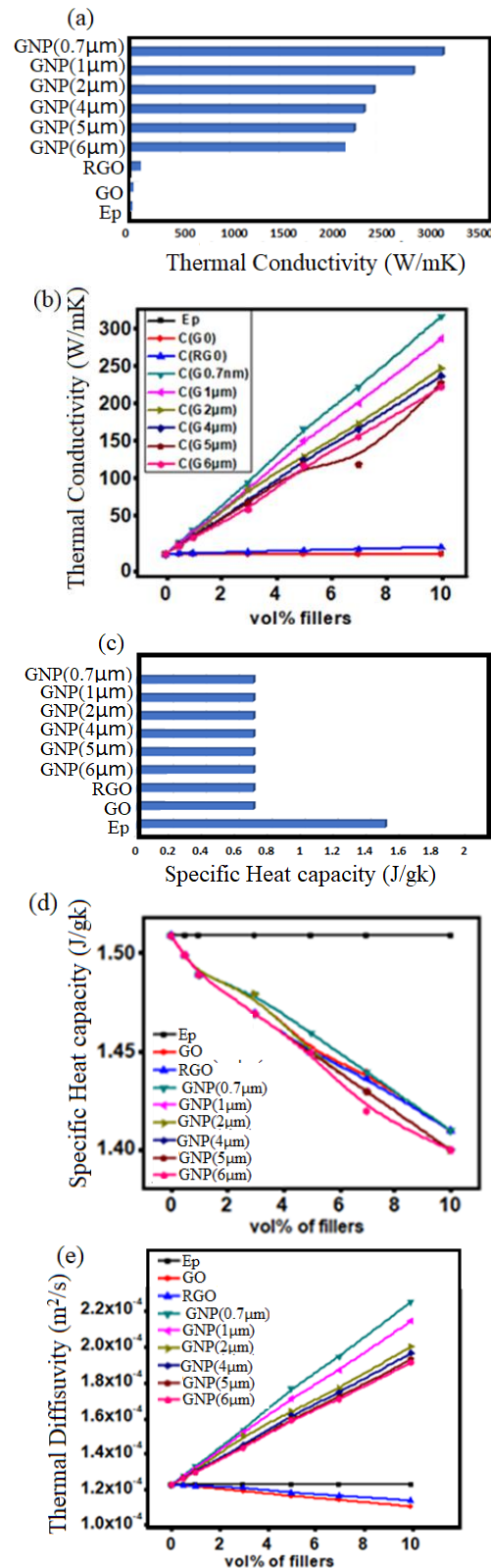
Figure 9. Thermal properties of various GNPs/Epoxy composites: **a)** Thermal conductivity of graphene oxide (GO), reduced graphene oxide

and various GNPs concerning thickness (0.7 nm, 1000 nm, 2000 nm, 4000 nm, 5000 nm, 6000 nm) composites, **b)** Thermal conductivity of epoxy/ graphene oxide (GO), reduced graphene oxide and various GNPs with respect to thickness (0.7 nm, 1000 nm, 2000 nm, 4000 nm, 5000 nm, 6000nm)/ epoxy composites, **c)** Specific heat capacity of graphene oxide (GO), reduced graphene oxide and various GNPs with respect to thickness (0.7 nm, 1000 nm, 2000 nm, 4000 nm, 5000 nm, 6000 nm), **d)** Specific heat capacity of epoxy/graphene oxide (GO), reduced graphene oxide and various GNPs with respect to the thickness in nm (0.7 nm, 1000 nm, 2000 nm, 4000 nm, 5000 nm, 6000 nm)/ epoxy composites, **e)** Thermal diffusivity of epoxy/ graphene oxide (GO), reduced graphene oxide and various GNPs with respect to the thickness in nm (0.7 nm, 1000 nm, 2000 nm, 4000 nm, 5000 nm, 6000 nm)/ epoxy composites.

4.4. Simulated thermal conductivity of BaTiO₃/epoxy nanocomposites

Thermal conductivity is related to thermal diffusivity as well as specific heat capacity and a decrease in thermal diffusivity improves thermal conductivity. Figure 10 presents the change in thermal conductivity of $BaTiO_3$ with respect to the diameter of $BaTiO_3$ and $BaTiO_3$/epoxy composites. It was found that the thermal conductivity of $BaTiO_3$/epoxy composites can be enhanced by increasing the vol% of $BaTiO_3$. Thermal conductivity of $BaTiO_3$ having a different diameter of particles is shown in Figure 10a. Figure 10 shows that the change of thermal conductivity is influenced by the diameter of BaTiO3 and the thermal conductivity can be improved by increasing the diameter of BaTiO3 particles.

Furthermore, Figure 10a also presents a comparison of thermal conductivity of BaTiO3/epoxy composites including different diameters of $BaTiO_3$ particles as well as content fillers, it confirms that the diameter of $BaTiO_3$ particles greatly influences thermal conductivity of simulated BaTiO3/epoxy composites, resulting in an increase of the thermal conductivity as a function of increasing diameter of the $BaTiO_3$ particle diameter. Additionally, a trend was observed for the thermal conductivity in epoxy composites. It was seen that the thermal conductivity enhances by increasing the fillers proportion as well as the size of BaTiO3 nanoplatelets (from nm to µm). We attribute this improvement to the uniform network between BaTiO3 particles.
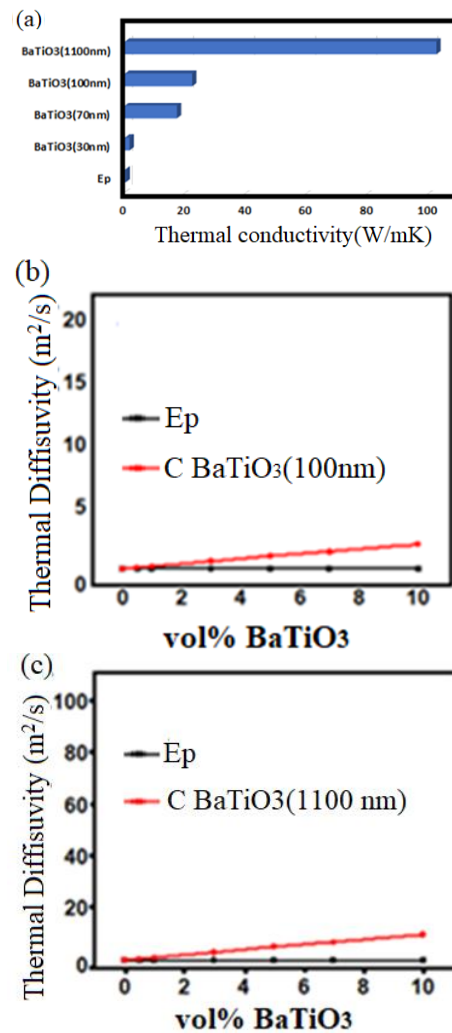

Figure 10. Thermal conductivity of $BaTiO_3$/Epoxy composites: **a)** Thermal conductivity of composites having various $BaTiO_3$ diameter (300 nm, 70 nm, 100 nm, 1100 nm) b) Thermal conductivity of $BaTiO_3$ with respect to diameter 300 nm, c) Thermal conductivity of $BaTiO_3$ with respect to diameter 70 nm, d) Comparative study of thermal conductivity of $BaTiO_3$ with respect to diameter 70 nm and GNPs (100nm), e) Comparative study of thermal conductivity of $BaTiO_3$ for diameter 1100 nm.

Figure 10b-c shows changes in the thermal diffusivity for $BaTiO_3$/epoxy composites for various amount of filler materials. The results showed a decrease in thermal diffusivity with increasing filler volume which seems to occur due to the increased mean free path. Thermal diffusivity of composites samples from $BaTiO_3$ with different diameter/ epoxy presents a decreasing tendency of thermal diffusivity (from lower to higher diameter) due to the greater mean free path of phonon-phonon in the case of higher diameter BaTiO3 and higher the speed and attenuation of a heat transfer in epoxy/BaTiO3 composites, it also proves the refractory behaviour of $BaTiO_3$.

Corresponding, Figure 11 shows the change in thermal diffusivity of neat epoxy vs BaTiO3 embedded epoxy for different particles sizes (100 nm and 300 nm) in different volume percentages.
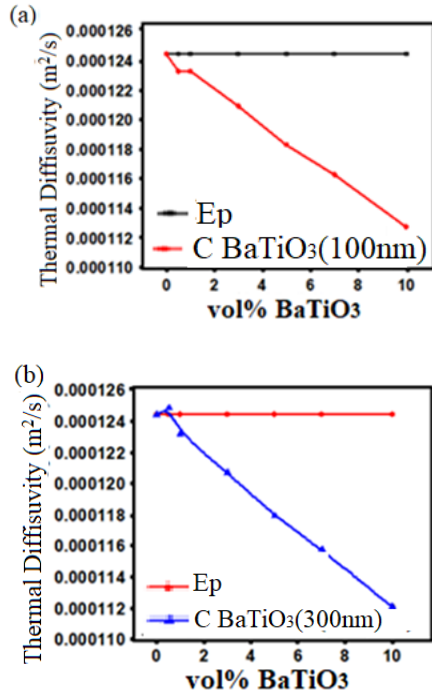

Figure 11. a) Thermal diffusivity of epoxy/ BaTiO$_3$ (100 nm diameter) composites, **b)** Thermal diffusivity of epoxy/ BaTiO$_3$ (300 nm diameter) composites

4.5. Relationship of simulated results by Bayesian analysis

Bayes' theorem is defined as a probability rule, which states different types of conditional probability density functions with respect to each other. Bayesian method of statistical inference helps to obtain a posterior (or updated) distribution by using prior information. The advancement in the theory as well as application of FE analysis methods have made it possible for application of Bayesian methods in reliability applications such as degradation behavior in a laser life test(Lindley, 1980), probabilistic risk problems as well as reliability of system (Rosner, 2020), system reliability and accelerated testing(van de Schoot et al., 2014).

Whenever, certain probabilities are known, the Bayes' theorem is used to find the other probabilities, the formula,

$$P\left(\frac{A}{B}\right) = \frac{P(A)P(B/A)}{P(B)} \qquad (6)$$

Equation (6) is the likelihood of event A is occurring when event B has happened;

Similarly,

$$P\left(\frac{B}{A}\right) = \frac{P(B)P(A/B)}{P(A)} \qquad (7)$$

Equation (7) is the likelihood of event B is occurring when event A has happened;

The Bayes' theorem can be written in the case of two or more cases of event A, than the probability of event B can be defined as equation 8:

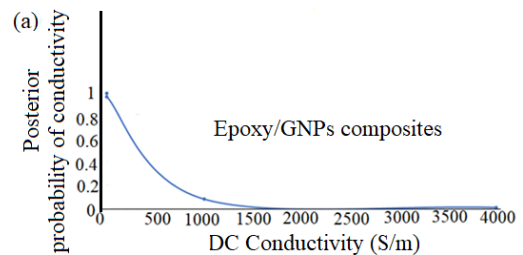$$P(B) = \frac{P(A)P\left(\frac{B}{A}\right) + P(Af)P(B/Af)}{P(A)} \qquad (8)$$

Wherein, P(Af) is the probability of the event A not occurring, P(Af)+P(A)=1 as either event A occurs, or it doesn't occur.

Finally, Bayes extended formula for probabilities of happening is shown in equation (9); it is useful to measure the chances, which is defined that the chance of a test is correct or wrong.

$$P\left(\frac{A}{B}\right) = \frac{P(A)P\left(\frac{B}{A}\right)}{P(A)P\left(\frac{B}{A}\right) + P(Af)P(B/Af)} \qquad (9)$$

This part of the paper describes and analyse electrical and thermal properties dataset of epoxy/graphene and epoxy/BaTiO$_3$ composites by using Bayesian model for probabilistic estimation. The Bayesian approach in which the goal is to find the probability distribution of the electrical conductivity, dielectric constant and thermal conductivity, as shown in Figure 12.

From this additional probabilistic analysis, it was found that the probability of DC conductivity, dielectric conductivity and thermal conductivity decreases with increasing simulated DC conductivity, dielectric constant and thermal conductivity of the composites respectively. It confirms that the properties of nanofillers do not completely participate in influencing the properties of composites, and several other parameters should also be responsible in the reduction of the properties of composites in compared to the pristine fillers' properties.
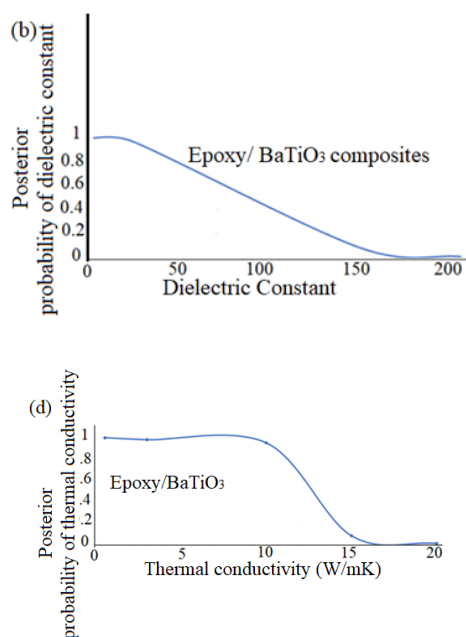
Figure 12. **a)** Posterior probability of DC conductivity of epoxy/ GNPs composites with respect to the DC conductivity of the simulated epoxy/GNPs composites, **b)** Posterior probability of Dielectric constant of epoxy/ BaTiO₃ composites with respect to the Dielectric constant of the simulated epoxy/ BaTiO₃ composites, **c)** Posterior probability of Thermal conductivity of epoxy/ GNPs composites with respect to the Thermal conductivity of the simulated epoxy/GNPs composites, d) Posterior probability of Thermal conductivity of epoxy/ BaTiO₃ composites with respect to the Thermal conductivity of the simulated epoxy/ BaTiO₃ composites.

Conclusions

In this study, the DC conductivity, dielectric constant, thermal diffusivity, specific heat capacity, and thermal conductivity values were numerically approximated using finite element analysis for a wide range of graphene and BaTiO3 reinforced epoxy nanocomposites. During the simulation, the geometry and distribution of graphene and its derivatives such as graphene oxide (GO), nanoplatelets (GNP) as well as BaTiO₃ were varied, and results were analysed. It was seen that the electrical and thermal properties of epoxy/GNPs and epoxy/BaTiO3 composites improves with an increase in the value of filler material, such as the DC conductivity of graphene oxide /epoxy composites was seen to be two times higher than the neat epoxy, and the DC conductivity of GNPs (1 nm) /epoxy composites was found to be several times higher than the neat epoxy. In general, all types of graphene/ epoxy composites showed large improvements in DC conductivity than the neat epoxy. The conductivity of composites has been related to the quantum tunneling of electrons

throughout the polymer matrix. The dielectric constant of graphene/epoxy composites improves by several orders of magnitude than the neat epoxy, for example, the dielectric constant of reduced graphene oxide (RGO) and graphene oxide (GO)/epoxy composites was seen to increase by several times. Also, the dielectric constant was correlated with the storage of charge between the fillers and matrix. The results showed that the thermal conductivity and diffusivity were enhanced by addition of GNPs e.g., the dimension of nanofillers and content of nanofillers. Additionally, the DC conductivity of BaTiO₃/epoxy composites were seen to increase by the inclusion of BaTiO₃ in the neat epoxy. As such all combinations of BaTiO₃/epoxy composites showed large improvement in the DC conductivity than the neat epoxy.

In summary, the thermal properties of epoxy/graphenes and epoxy/BaTiO₃ were simulated and it was seen that graphene based epoxy nanocomposites showed superior enhancement in the thermal properties compared to BaTiO₃ based epoxy nanocomposites. The best thermal conductivity of GNP 0.7nm/epoxy composites with 10vol% filler was found to be about 307 W m^{-1} K^{-1}.

Conflict of interest

The authors declare to have no conflict of interest.

References

Atif, R., Shyha, I., & Inam, F. (2016). Mechanical, thermal, and electrical properties of graphene-epoxy nanocomposites-A review. In *Polymers*. https://doi.org/10.3390/polym8080281

Barber, P., Balasubramanian, S., Anguchamy, Y., Gong, S., Wibowo, A., Gao, H., Ploehn, H. J., & Loye, H. C. Zur. (2009). Polymer composite and nanocomposite dielectric materials for pulse power energy storage. *Materials.* https://doi.org/10.3390/ma2041697

Bauhofer, W., & Kovacs, J. Z. (2009). A review and analysis of electrical percolation in carbon nanotube polymer composites. *Composites Science and Technology*, *69*(10), 1486–1498. https://doi.org/10.1016/j.compscitech.2008.06.018

Bikky, R., Badi, N., & Bensaoula, A. (2010). Effective Medium Theory of Nanodielectrics for Embedded Energy Storage Capacitors. *Comsol.De.*

Caradonna, A., Badini, C., Padovano, E., & Pietroluongo, M. (2019). Electrical and thermal conductivity of epoxy-carbon filler composites processed by calendaring. *Materials.* https://doi.org/10.3390/ma12091522

Carotenuto, G., Romeo, V., Cannavaro, I., Roncato, D., Martorana, B., & Gosso, M. (2012). Graphene-polymer composites. *IOP Conference Series: Materials Science and Engineering.* https://doi.org/10.1088/1757-899X/40/1/012018

Chikhi, M., Agoudjil, B., Haddadi, M., & Boudenne, A. (2013). Numerical modelling of the effective thermal conductivity of heterogeneous materials. *Journal of Thermoplastic Composite Materials.* https://doi.org/10.1177/0892705711424921

Cho, K. S. (2016). Polymer physics. In *Springer Series in Materials Science.* https://doi.org/10.1007/978-94-017-7564-9_4

Cho, S. D., Lee, S. Y., Hyun, J. G., & Paik, K. W. (2005). Comparison of theoretical predictions and experimental values of the dielectric constant of epoxy/BaTiO3 composite embedded capacitor films. *Journal of Materials Science: Materials in Electronics.* https://doi.org/10.1007/s10854-005-6454-3

Ekanath, D. M., Badi, N., & Bensaoula, A. (2011). Modeling and Simulation of Artificial Core-Shell Based Nanodielectrics for Electrostatic Capacitors Applications. *Comsol Conference.*

Friedrich, K., & Almajid, A. A. (2013). Manufacturing Aspects of Advanced Polymer Composites for Automotive Applications. *Applied Composite Materials*, *20*(2), 107–128. https://doi.org/10.1007/s10443-012-9258-7

Galpaya, D., Wang, M., Liu, M., Motta, N., Waclawik, E., & Yan, C. (2012). Recent Advances in Fabrication and Characterization of Graphene-Polymer Nanocomposites. *Graphene*, *01*(02), 30–49. https://doi.org/10.4236/graphene.2012.12005

Gresil, M., Wang, Z., Poutrel, Q. A., & Soutis, C. (2017). Thermal Diffusivity Mapping of Graphene Based Polymer Nanocomposites. *Scientific Reports.* https://doi.org/10.1038/s41598-017-05866-0

Hass, J., De Heer, W. A., & Conrad, E. H. (2008). The growth and morphology of epitaxial multilayer graphene. In *Journal of Physics Condensed Matter.* https://doi.org/10.1088/0953-8984/20/32/323202

Hou, H., Dai, W., Yan, Q., Lv, L., Alam, F. E., Yang, M., Yao, Y., Zeng, X., Xu, J. Bin, Yu, J., Jiang, N., & Lin, C. Te. (2018). Graphene size-dependent modulation of graphene frameworks contributing to the superior thermal conductivity of epoxy composites. *Journal of Materials Chemistry A.* https://doi.org/10.1039/c8ta03937b

Jarosinski, L., Rybak, A., Gaska, K., Kmita, G., Porebska, R., & Kapusta, C. (2017). Enhanced thermal conductivity of graphene nanoplatelets epoxy composites. *Materials Science- Poland.* https://doi.org/10.1515/msp-2017-0028

Kargar, F., Barani, Z., Salgado, R., Debnath, B., Lewis, J. S., Aytan, E., Lake, R. K., & Balandin, A. A. (2018). Thermal Percolation Threshold and Thermal Properties of Composites with High Loading of Graphene and Boron Nitride Fillers. *ACS Applied Materials and Interfaces.* https://doi.org/10.1021/acsami.8b16616

Kim, D. S., Baek, C., Ma, H. J., & Kim, D. K. (2016). Enhanced dielectric permittivity of BaTiO3/epoxy resin composites by particle alignment. *Ceramics International.* https://doi.org/10.1016/j.ceramint.2016.01.103

Korattanawittaya, S., Petcharoen, K., Sangwan, W., Tangboriboon, N., Wattanakul, K., & Sirivat, A. (2017). Durable compliant electrode based on graphene and natural rubber. *Polymer Engineering and Science.* https://doi.org/10.1002/pen.24392

Kultzow, R., & Mainguy, B. (2001). Low dielectric constant and low shrinkage epoxy system for power electronics applications. *Proceedings of the Electrical/Electronics Insulation Conference.* https://doi.org/10.1109/EEIC.2001.965629

Lewis, J. S., Barani, Z., Magana, A. S., Kargar, F., & Balandin, A. A. (2019). Thermal and electrical conductivity control in hybrid composites with graphene and boron nitride fillers. *Materials Research Express.* https://doi.org/10.1088/2053-1591/ab2215

Li, Y., Zhang, H., Porwal, H., Huang, Z., Bilotti, E., & Peijs, T. (2017). Mechanical, electrical and thermal properties of in-situ exfoliated graphene/epoxy nanocomposites. *Composites*

Part A: Applied Science and Manufacturing. https://doi.org/10.1016/j.compositesa.2017.01.007

Lindley, D. V. (1980). Approximate Bayesian methods. *Trabajos de Estadistica Y de Investigacion Operativa*, *31*(1), 223–245. https://doi.org/10.1007/BF02888353

Luo, S., Shen, Y., Yu, S., Wan, Y., Liao, W. H., Sun, R., & Wong, C. P. (2017). Construction of a 3D-BaTiO3 network leading to significantly enhanced dielectric permittivity and energy storage density of polymer composites. *Energy and Environmental Science.* https://doi.org/10.1039/c6ee03190k

Marra, F., D'Aloia, A. G., Tamburrano, A., Ochando, I. M., De Bellis, G., Ellis, G., & Sarto, M. S. (2016). Electromagnetic and dynamic mechanical properties of epoxy and vinylester-based composites filled with graphene nanoplatelets. *Polymers.* https://doi.org/10.3390/polym8080272

Marsden, A. J., Papageorgiou, D. G., Vallés, C., Liscio, A., Palermo, V., Bissett, M. A., Young, R. J., & Kinloch, I. A. (2018). Electrical percolation in graphene-polymer composites. In *2D Materials.* https://doi.org/10.1088/2053-1583/aac055

Mather, P. T., Luo, X., & Rousseau, I. A. (2009). Shape memory polymer research. In *Annual Review of Materials Research.* https://doi.org/10.1146/annurev-matsci-082908-145419

McGrail, B. T., Sehirlioglu, A., & Pentzer, E. (2015). Polymer composites for thermoelectric applications. *Angewandte Chemie - International Edition.* https://doi.org/10.1002/anie.201408431

Mekala, R., & Badi, N. (2013). Modeling and Simulation of High Permittivity Core-shell Ferroelectric Polymers for Energy Storage Solutions. *COMSOL Conference.*

Ming, P., Zhang, Y., Bao, J., Liu, G., Li, Z., Jiang, L., & Cheng, Q. (2015). Bioinspired highly electrically conductive graphene-epoxy layered composites. *RSC Advances.* https://doi.org/10.1039/c5ra00233h

Oladele, I. O., Omotosho, T. F., & Adediran, A. A. (2020). Polymer-Based Composites: An Indispensable Material for Present and Future Applications. *International Journal of Polymer Science*, *2020*, 1–12. https://doi.org/10.1155/2020/8834518

Pant, H. C., Patra, M. K., Verma, A., Vadera, S. R., & Kumar, N. (2006). Study of the dielectric properties of barium titanate-polymer composites. *Acta Materialia.* https://doi.org/10.1016/j.actamat.2006.02.031

Pathak, A. K., Borah, M., Gupta, A., Yokozeki, T., & Dhakate, S. R. (2016). Improved mechanical properties of carbon

fiber/graphene oxide-epoxy hybrid composites. *Composites Science and Technology.* https://doi.org/10.1016/j.compscitech.2016.09.007

Phan, T. T. M., Chu, N. C., Luu, V. B., Nguyen Xuan, H., Martin, I., & Carriere, P. (2016). The role of epoxy matrix occlusions within BaTiO3 nanoparticles on the dielectric properties of functionalized BaTiO3/epoxy nanocomposites. *Composites Part A: Applied Science and Manufacturing.* https://doi.org/10.1016/j.compositesa.2016.08.018

Phan, T. T. M., Chu, N. C., Luu, V. B., Nguyen Xuan, H., Pham, D. T., Martin, I., & Carrière, P. (2016). Enhancement of polarization property of silane-modified BaTiO3 nanoparticles and its effect in increasing dielectric property of epoxy/BaTiO3 nanocomposites. *Journal of Science: Advanced Materials and Devices.* https://doi.org/10.1016/j.jsamd.2016.04.005

Popielarz, R., & Chiang, C. K. (2007). Polymer composites with the dielectric constant comparable to that of barium titanate ceramics. *Materials Science and Engineering B: Solid-State Materials for Advanced Technology.* https://doi.org/10.1016/j.mseb.2007.01.035

R. Byron Bird Warren E. Stewart Edwin N. Lightfoo, Bird, R. B., Stewart, W. E., & Lightfoot, E. N. (2006). Transport Phenomena, Revised 2nd Edition. *John Wiley & Sons, Inc.*

Rosner, G. L. (2020). Bayesian Methods in Regulatory Science. *Statistics in Biopharmaceutical Research*, *12*(2), 130–136. https://doi.org/10.1080/19466315.2019.1668843

Schumacher, J., Fideu, P., Ziegmann, G., & Herrmann, A. (2009). A Consistent Environment for the Numerical Prediction of the Properties of Composite Materials. *COMSOL Conference.*

Shahil, K. M. F., & Balandin, A. A. (2012a). Graphene-multilayer graphene nanocomposites as highly efficient thermal interface materials. *Nano Letters.* https://doi.org/10.1021/nl203906r

Shahil, K. M. F., & Balandin, A. A. (2012b). Thermal properties of graphene and multilayer graphene: Applications in thermal interface materials. *Solid State Communications.* https://doi.org/10.1016/j.ssc.2012.04.034

Tang, G., Jiang, Z. G., Li, X., Zhang, H. Bin, Hong, S., & Yu, Z. Z. (2014). Electrically conductive rubbery epoxy/diamine-functionalized graphene nanocomposites with improved mechanical properties. *Composites Part B:*

Engineering. https://doi.org/10.1016/j.compositesb.2014.08.013

Tomer, V., Polizos, G., Manias, E., & Randall, C. A. (2010). Epoxy-based nanocomposites for electrical energy storage. I: Effects of montmorillonite and barium titanate nanofillers. *Journal of Applied Physics*. https://doi.org/10.1063/1.3487275

van de Schoot, R., Kaplan, D., Denissen, J., Asendorpf, J. B., Neyer, F. J., & van Aken, M. A. G. (2014). A Gentle Introduction to Bayesian Analysis: Applications to Developmental Research. *Child Development*, *85*(3), 842–860. https://doi.org/10.1111/cdev.12169

Wang, Z., Nelson, J. K., Koratkar, N., Schadler, L. S., Hillborg, H., & Zhao, S. (2011). Dielectric properties of electrospun barium titanate fibers/graphene/ silicone rubber composites. *Annual Report - Conference on Electrical Insulation and Dielectric Phenomena, CEIDP*. https://doi.org/10.1109/CEIDP.2011.6232738

Wang, Zepu, Nelson, J. K., Miao, J., Linhardt, R. J., Schadler, L. S., Hillborg, H., & Zhao, S. (2012). Effect of high aspect ratio filler on dielectric properties of polymer composites: A study on barium titanate fibers and graphene platelets. *IEEE Transactions on Dielectrics and Electrical Insulation*.

https://doi.org/10.1109/TDEI.2012.6215100

Yousefi, N., Sun, X., Lin, X., Shen, X., Jia, J., Zhang, B., Tang, B., Chan, M., & Kim, J. K. (2014). Highly aligned graphene/polymer nanocomposites with excellent dielectric properties for high-performance electromagnetic interference shielding. *Advanced Materials*, *26*(31), 5480–5487. https://doi.org/10.1002/adma.201305293

Zandiatashbar, A., Lee, G. H., An, S. J., Lee, S., Mathew, N., Terrones, M., Hayashi, T., Picu, C. R., Hone, J., & Koratkar, N. (2014). Effect of defects on the intrinsic strength and stiffness of graphene. *Nature Communications*. https://doi.org/10.1038/ncomms4186

Zhang, C., Chi, Q., Dong, J., Cui, Y., Wang, X., Liu, L., & Lei, Q. (2016). Enhanced dielectric properties of poly(vinylidene fluoride) composites filled with nano iron oxide-deposited barium titanate hybrid particles. *Scientific Reports*. https://doi.org/10.1038/srep33508

Zhao, S., Chang, H., Chen, S., Cui, J., & Yan, Y. (2016). High-performance and multifunctional epoxy composites filled with epoxide-functionalized graphene. *European Polymer Journal*. https://doi.org/10.1016/j.eurpolymj.2016.09.036